Neutron Powder Diffraction Study on the Crystal and Magnetic Structures of $BiCrO_3$

Alexei A. Belik,*,† Satoshi Iikubo,‡ Katsuaki Kodama,‡ Naoki Igawa,‡ Shinichi Shamoto,‡ and Eiji Takayama-Muromachi†

International Center for Materials Nanoarchitectonics (MANA), National Institute for Materials Science (NIMS), 1-1 Namiki, Tsukuba, Ibaraki 305-0044, Japan, and Quantum Beam Science Directorate, Japan Atomic Energy Agency, Tokai, Ibaraki 319-1195, Japan

Received February 5, 2008. Revised Manuscript Received March 21, 2008

The crystal and magnetic structures of polycrystalline $BiCrO_3$ were determined by the Rietveld method from neutron diffraction data measured at temperatures from 7 to 490 K. $BiCrO_3$ crystallizes in the orthorhombic system above 420 K (space group *Pnma*; $Z = 4$; $a = 5.54568(12)$ Å, $b = 7.7577(2)$ Å, and $c = 5.42862(12)$ Å at 490 K) in the $GdFeO_3$-type structure. Below 420 K down to 7 K, a monoclinic structure is stable with *C*2/*c* symmetry ($a = 9.4641(4)$ Å, $b = 5.4790(2)$ Å, $c = 9.5850(4)$ Å, and $\beta = 108.568(3)°$ at 7 K). A possible model for antiferromagnetic order below $T_N = 109$ K is proposed with a propagation vector of $\mathbf{k} = (0, 0, 0)$. In this model, magnetic moments of Cr^{3+} ions are coupled antiferromagnetically in all directions, forming a G-type antiferromagnetic structure. Refined magnetic moments at 7, 50, and 80 K are $2.55(2)\mu_B$, $2.43(2)\mu_B$, and $2.09(2)\mu_B$, respectively. The structure refinements revealed no deviation from stoichiometry in $BiCrO_3$.

Introduction

Bi containing perovskites have attracted much attention during the past decade as multiferroic and lead-free ferroelectric materials because of the presence of the stereochemically active lone electron pair of a Bi^{3+} ion.[1–9] In multiferroic systems, two or all three of (anti)ferroelectricity, (anti)ferromagnetism, and ferroelasticity characteristics are observed in the same phase.[10] Such systems seem to be rare in nature, but they are quite interesting because of their possible applications in devices (e.g., multiple-state memory elements)[10] and new basic physics (e.g., ferroelectricity induced by charge ordering and spiral magnetic ordering).[11,12]

Despite of the presence of Bi^{3+} ions in simple $BiMO_3$ systems (M = transition metals), only $BiFeO_3$ and $BiCoO_3$ definitely have polar structures,[13,14] and ferroelectric properties of $BiFeO_3$ have been shown experimentally in a large number of works.[13] $BiNiO_3$ crystallizes in the centrosymmetric space group $P2_1/c$.[15] Ideal $BiMnO_3$ should crystallize in the centrosymmetric space group *C*2/*c*.[16] Neutron powder diffraction data showed that average and even local structures of $BiMnO_3$ are indeed very well-described by the *C*2/*c* model.[17–19] In terms of convergent-beam electron diffraction, the space group of bulk $BiMnO_3$ also was determined to be *C*2/*c*.[20] However, careful selected-area electron diffraction studies showed a long-range ordered structure with *C*2 symmetry and a short-range ordered structure with *P*2 or $P2_1$ symmetry.[20] The local symmetry of bulk $BiMnO_3$ was

* Author to whom correspondence should be addressed. E-mail: Alexei.BELIK@nims.go.jp.
† MANA-NIMS.
‡ Japan Atomic Energy Agency.

(1) Ramesh, R.; Spaldin, N. A. *Nat. Mater.* **2007**, *6*, 21.
(2) Eerenstein, W.; Mathur, N. D.; Scott, J. F. *Nature (London, U.K.)* **2006**, *442*, 759.
(3) Khomskii, D. I. *J. Magn. Magn. Mater.* **2006**, *306*, 1.
(4) Fiebig, M. *J. Phys. D: Appl. Phys.* **2005**, *38*, 123.
(5) Baettig, P.; Ederer, C.; Spaldin, N. A. *Phys. Rev. B: Condens. Matter Mater. Phys.* **2005**, *72*, 214105.
(6) (a) Azuma, M.; Takata, K.; Saito, T.; Ishiwata, S.; Shimakawa, Y.; Takano, M. *J. Am. Chem. Soc.* **2005**, *127*, 8889. (b) Bridges, C. A.; Allix, M.; Suchomel, M. R.; Kuang, X. J.; Sterianou, I.; Sinclair, D. C.; Rosseinsky, M. J. *Angew. Chem., Int. Ed.* **2007**, *46*, 8787. (c) Hughes, H.; Allix, M. M. B.; Bridges, C. A.; Claridge, J. B.; Kuang, X. J.; Niu, H. J.; Taylor, S.; Song, W. H.; Rosseinsky, M. J. *J. Am. Chem. Soc.* **2005**, *127*, 13790.
(7) Ishiwata, S.; Azuma, M.; Takano, M. *Chem. Mater.* **2007**, *19*, 1964.
(8) Zylberberg, J.; Belik, A. A.; Takayama-Muromachi, E.; Ye, Z. G. *Chem. Mater.* **2007**, *19*, 6385.
(9) Baettig, P.; Schelle, C. F.; LeSar, R.; Waghmare, U. V.; Spaldin, N. A. *Chem. Mater.* **2005**, *17*, 1376.
(10) Hill, N. A. *J. Phys. Chem. B* **2000**, *104*, 6694.
(11) Ikeda, N.; Ohsumi, H.; Ohwada, K.; Ishii, K.; Inami, T.; Kakurai, K.; Murakami, Y.; Yoshii, K.; Mori, S.; Horibe, Y.; Kito, H. *Nature (London, U.K.)* **2005**, *436*, 1136.
(12) Kimura, T.; Goto, T.; Shintani, H.; Ishizaka, K.; Arima, T.; Tokura, Y. *Nature (London, U.K.)* **2003**, *426*, 55.
(13) Wang, J.; Neaton, J. B.; Zheng, H.; Nagarajan, V.; Ogale, S. B.; Liu, B.; Viehland, D.; Vaithyanathan, V.; Schlom, D. G.; Waghmare, U. V.; Spaldin, N. A.; Rabe, K. M.; Wuttig, M.; Ramesh, R. *Science (Washington, DC, U.S.)* **2003**, *299*, 1719.
(14) Belik, A. A.; Iikubo, S.; Kodama, K.; Igawa, N.; Shamoto, S.; Niitaka, S.; Azuma, M.; Shimakawa, Y.; Takano, M.; Izumi, F.; Takayama-Muromachi, E. *Chem. Mater.* **2006**, *18*, 798.
(15) Ishiwata, S.; Azuma, M.; Takano, M.; Nishibori, E.; Takata, M.; Sakata, M.; Kato, K. *J. Mater. Chem.* **2002**, *12*, 3733.
(16) Baettig, P.; Seshadri, R.; Spaldin, N. A. *J. Am. Chem. Soc.* **2007**, *129*, 9854.
(17) Belik, A. A.; Iikubo, S.; Yokosawa, T.; Kodama, K.; Igawa, N.; Shamoto, S.; Azuma, M.; Takano, M.; Kimoto, K.; Matsui, Y.; Takayama-Muromachi, E. *J. Am. Chem. Soc.* **2007**, *129*, 971.
(18) Montanari, E.; Calestani, G.; Righi, L.; Gilioli, E.; Bolzoni, F.; Knight, K. S.; Radaelli, P. G. *Phys. Rev. B: Condens. Matter Mater. Phys.* **2007**, *75*, 220101.
(19) Kodama, K.; Iikubo, S.; Shamoto, S.; Belik, A. A.; Takayama-Muromachi, E. *J. Phys. Soc. Jpn.* **2007**, *76*, 124605.
(20) Yokosawa, T.; Belik, A. A.; Asaka, T.; Kimoto, K.; Takayama-Muromachi, E.; Matsui, Y. *Phys. Rev. B: Condens. Matter Mater. Phys.* **2008**, *77*, 24111.

10.1021/cm800375d CCC: $40.75
Published on Web 05/10/2008

confirmed to be $P2$ or $P2_1$ by atomic pair distribution function analysis.[19] In ref 21, it was suggested that $BiCrO_3$ has $C2$ symmetry by analogy with $BiMnO_3$. However, recent electron diffraction studies showed that $BiCrO_3$ crystallizes in the centrosymmetric space group $C2/c$.[20] Among simple $BiMO_3$ systems with nonmagnetic M atoms, $BiAlO_3$ and $BiInO_3$ crystallize in polar structures,[22,23] and ferroelectric properties of $BiAlO_3$ were demonstrated experimentally.[8] $BiScO_3$ adopts the same structure as $BiCrO_3$ with the space group $C2/c$.[20,24]

Crystal structures of $BiAlO_3$, $BiScO_3$, and $BiInO_3$ and magnetic and crystal structures of $BiMnO_3$, $BiFeO_3$, $BiCoO_3$, and $BiNiO_3$ were investigated using neutron and X-ray diffraction. $BiMnO_3$ is a ferromagnet below $T_C = 100$ K.[18,25] $BiCoO_3$ is a C-type antiferromagnet below $T_N = 470$ K,[14] and $BiNiO_3$ is a G-type (canted) antiferromagnet with $T_N = 300$ K.[15,26,27] $BiFeO_3$ is also an antiferromagnet but with a more complicated magnetic structure.[28] Among $BiMO_3$, only for $BiCrO_3$ have the crystal and magnetic structures not been reported yet. There is a structural phase transition in $BiCrO_3$ above 420 K from a monoclinic to orthorhombic structure.[21,29,30] The long-range antiferromagnetic order with weak ferromagnetism occurs below $T_N = 109$ K. Four anomalies of magnetic origin were found near 40, 75, 109, and 111 K in $BiCrO_3$.[30]

In this work, we determined the crystal and magnetic structures of $BiCrO_3$ by the Rietveld method from neutron powder diffraction data measured at 7, 50, 80, 130, and 490 K. Neutron diffraction unambiguously confirmed the onset of long-range G-type antiferromagnetic order below $T_N = 109$ K, showed that the magnetic structure does not change down to 7 K, and allowed us to acquire detailed structural information concerning $BiCrO_3$ in a wide temperature range.

Experimental Procedures

Synthesis. Mixtures of Bi_2O_3 (99.99%) and Cr_2O_3 (99.9%) with an amount-of-substance ratio of 1:1 were placed in Au capsules and treated at 6 GPa in a belt-type high-pressure apparatus at 1653 K for 60−70 min (heating rate of 140 K/min).[30] After heat treatment, the samples were quenched to room temperature (RT), and the pressure was slowly released. The resultant samples were khaki-green dense pellets. The procedure was repeated 7 times to produce ~5 g of the sample.

Neutron Powder Diffraction Experiments and Structure Refinements. Neutron powder diffraction data of $BiCrO_3$ were collected at 7, 50, 80, 130, and 490 K with the high-resolution powder diffractometer (HRPD) installed at the JRR-3 M reactor in JAEA, Tokai, Japan. The incident neutron wavelength was 1.8233(10) Å. Approximately 5 g of the sample was contained in a V holder (diameter of 6.0 mm) filled with He. A cryostat (or a furnace) containing the holder was slowly oscillated during the measurement. The data were taken with a step of ca. 0.05° in a 2θ range between 2.5 and 162° with 64 ^{3}He detectors.

The neutron powder diffraction data were analyzed by the Rietveld method with RIETAN-2000.[31] The background was represented by an eighth-order Legendre polynomial. The pseudo-Voigt function of Toraya[32] was used as a profile function (we refined 6 profile parameters). Isotropic atomic displacement parameters, B, with the isotropic Debye−Waller factor represented as $\exp(-B \sin^2\theta/\lambda^2)$ were assigned to all the sites. Bound coherent scattering lengths, b_c, used for the structure refinements were 8.532 fm (Bi), 3.635 fm (Cr), and 5.803 fm (O).[33] Coefficients for analytical approximations to the magnetic form factor of Cr^{3+} were taken from ref 34. A partial profile relaxation technique[31] was applied to the strongest 004, 400, −222, 222, and −404 reflections to improve fits in these reflections in the final refinements.

Neutron diffraction data showed the presence of an impurity, Cr_2O_3. For the impurity of Cr_2O_3, we refined a scale factor and lattice parameters (a and c), fixing its structural parameters. The mass percentage of Cr_2O_3 in the $BiCrO_3$ sample was calculated to be ~1%. The neutron diffraction pattern at 490 K showed additional reflections from a furnace (Cu and very weak reflections from Al).[17] Cu was taken into account during the refinement.

Results and Discussion

All the reflections of $BiCrO_3$ at 490 K could be indexed in an orthorhombic system with $a \approx 5.5457$ Å, $b \approx 7.7577$ Å, and $c \approx 5.4286$ Å. Reflection conditions derived from the indexed reflections were $k + l = 2n$ for $0kl$, $h = 2n$ for $hk0$ and $h00$, $k = 2n$ for $0k0$, and $l = 2n$ for $00l$, affording possible space groups $Pnma$ (No. 62, centrosymmetric) and $Pn2_1a$ (No. 33, noncentrosymmetric).[35] Therefore, for initial fractional coordinates in the Rietveld analysis of $BiCrO_3$, we used those of the $GdFeO_3$-type compounds with space group $Pnma$.[36] Attempts to refine the structure in space group $Pn2_1a$ did not improve the fit.

Table 1 gives fractional coordinates, B parameters, lattice parameters, and R factors resulting from the Rietveld refinement. Bond lengths (l), angles (φ), and bond-valence sums (BVS)[37] are given in Table 2. Figure 1a displays observed, calculated, and difference neutron diffraction patterns at 490 K.

(21) Niitaka, S.; Azuma, M.; Takano, M.; Nishibori, E.; Takata, M.; Sakata, M. *Solid State Ionics* **2004**, *172*, 557.
(22) Belik, A. A.; Wuernisha, T.; Kamiyama, T.; Mori, K.; Maie, M.; Nagai, T.; Matsui, Y.; Takayama-Muromachi, E. *Chem. Mater.* **2006**, *18*, 133.
(23) Belik, A. A.; Stefanovich, S. Y.; Lazoryak, B. I.; Takayama-Muromachi, E. *Chem. Mater.* **2006**, *18*, 1964.
(24) Belik, A. A.; Iikubo, S.; Kodama, K.; Igawa, N.; Shamoto, S.; Maie, M.; Nagai, T.; Matsui, Y.; Stefanovich, S. Y.; Lazoryak, B. I.; Takayama-Muromachi, E. *J. Am. Chem. Soc.* **2006**, *128*, 706.
(25) Moreira dos Santos, A.; Cheetham, A. K.; Atou, T.; Syono, Y.; Yamaguchi, Y.; Ohoyama, K.; Chiba, H.; Rao, C. N. R. *Phys. Rev. B: Condens. Matter Mater. Phys.* **2002**, *66*, 64425.
(26) Azuma, M.; Carlsson, S.; Rodgers, J.; Tucker, M. G.; Tsujimoto, M.; Ishiwata, S.; Isoda, S.; Shimakawa, Y.; Takano, M.; Attfield, J. P. *J. Am. Chem. Soc.* **2007**, *129*, 14433.
(27) Carlsson, S. J. E.; Azuma, M.; Shimakawa, Y.; Takano, M.; Hewat A.; Attfield, J. P. *J. Solid State Chem.* **2008,***181,*611.
(28) (a) Przenioslo, R.; Palewicz, A.; Regulski, M.; Sosnowska, I.; Ibberson, R. M.; Knight, K. S. *J. Phys.: Condens. Matter* **2006**, *18*, 2069. (b) Przenioslo, R.; Regulski, M.; Sosnowska, I. *J. Phys. Soc. Jpn.* **2006**, *75*, 84718.
(29) Sugawara, F.; Iiida, S.; Syono, Y.; Akimoto, S. *J. Phys. Soc. Jpn.* **1968**, *25*, 1553.
(30) Belik, A. A.; Tsujii, N.; Suzuki, H.; Takayama-Muromachi, E. *Inorg. Chem.* **2007**, *46*, 8746.
(31) Izumi, F.; Ikeda, T. *Mater. Sci. Forum* **2000**, *321−324*, 198.
(32) Toraya, H. *J. Appl. Crystallogr.* **1990**, *23*, 485.
(33) Sears, V. F. *International Tables for Crystallography*, 3rd ed.;Kluwer: Dordrecht, The Netherlands, 2004; *Vol. C*, pp 445−452..
(34) Brown, P. J. *International Tables for Crystallography*, 3rd ed.; Kluwer: Dordrecht, The Netherlands, 2004; *Vol. C*, p 454.
(35) Hahn, T. *International Tables for Crystallography*, 5th ed.; Kluwer: Dordrecht, The Netherlands, 2002; *Vol. A*, p 52.
(36) Oikawa, K.; Kamiyama, T.; Hashimoto, T.; Shimojyo, Y.; Morii, Y. *J. Solid State Chem.* **2000**, *154*, 524.
(37) Brese, R. E.; O'Keeffe, M. *Acta Crystallogr., Sect. B: Struct. Sci.* **1991**, *47*, 192.

Table 1. Structure Parameters of $BiCrO_3$ at 490 K[a]

site	Wyckoff position	x	y	z	B (Å^2)
Bi	4*c*	0.0429(2)	0.25	0.9954(3)	1.02(3)
Cr	4*b*	0	0	0.5	0.46(4)
O1	4*c*	0.4783(3)	0.25	0.0798(3)	0.65(3)
O2	8*d*	0.2959(2)	0.03958(16)	0.7030(2)	1.01(3)

[a] Space group *Pnma* (No. 62); $Z = 4$; $a = 5.54568(12)$ Å, $b = 7.7577(2)$ Å, $c = 5.42862(12)$ Å; $V = 233.548(9)$ Å^3; $R_{wp} = 4.12\%$ ($S = R_{wp}/R_e = 1.27$), $R_p = 3.12\%$, $R_B = 2.59\%$, and $R_F = 1.41\%$. Occupation of all sites is unity.

Table 2. Bond Lengths (l, Å), Angles (φ, deg) BVS in $BiCrO_3$ at 490 K

bonds	l	bonds and angles	l or φ
Bi−O1	2.334(2)	Cr−O1 (×2)	1.991(1)
Bi−O2 (×2)	2.388(2)	Cr−O2 (×2)	1.994(1)
Bi−O1a	2.458(2)	Cr−O2a (×2)	2.000(1)
Bi−O2a (×2)	2.668(2)	BVS(Cr)	2.88
Bi−O2b (×2)	2.674(2)	Cr−O1−Cr (×2)	153.9(1)
Bi−O1b	3.143(2)	Cr−O2−Cr (×4)	152.6(1)
Bi−O1c	3.164(2)		
BVS(Bi)	2.76		

Below 420 K, a monoclinic structure of $BiCrO_3$ is stable.[21] Convergent-beam and selected-area electron diffraction studies showed that the crystal symmetry of the monoclinic phase is *C*2/*c*.[20] Therefore, for initial fractional coordinates in the Rietveld analysis of $BiCrO_3$ between 7 and 130 K, we used those of $BiMnO_3$ in space group *C*2/*c*.[17]

Below T_N (at 7, 50, and 80 K), no new reflections appeared, but a few reflections significantly changed their intensities and could not be fit with the nuclear model (Figure 2b). They corresponded to magnetic scattering due to antiferromagnetic order. The magnetic reflections could be

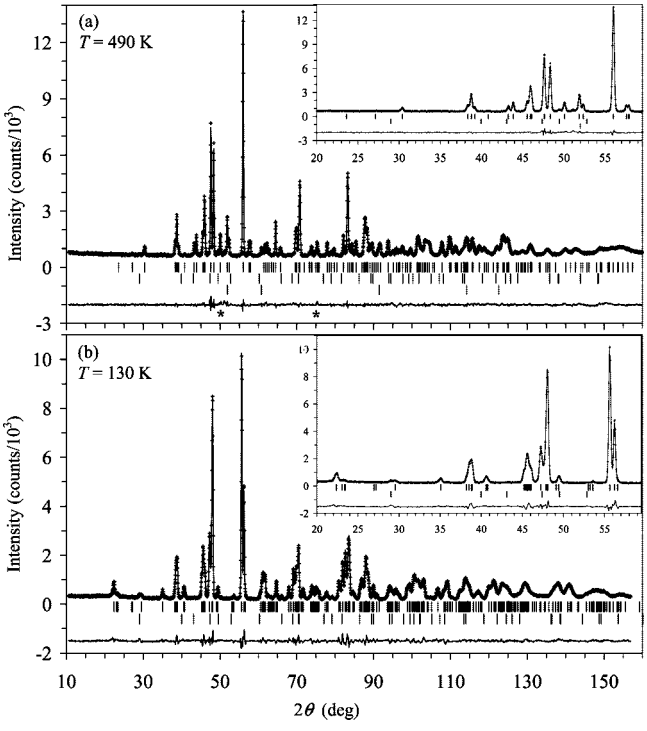

Figure 1. Observed (crosses), calculated (solid line), and difference patterns resulting from the Rietveld analysis of the neutron powder diffraction data for $BiCrO_3$ at (a) 490 K and (b) 130 K. Bragg reflections are indicated by tick marks. The lower tick marks are given for reflections from Cr_2O_3. In panel a, the third row of tick marks is given for reflections from a furnace, Cu; reflections from Al are shown with asterisks. Insets depict the enlarged fragments.

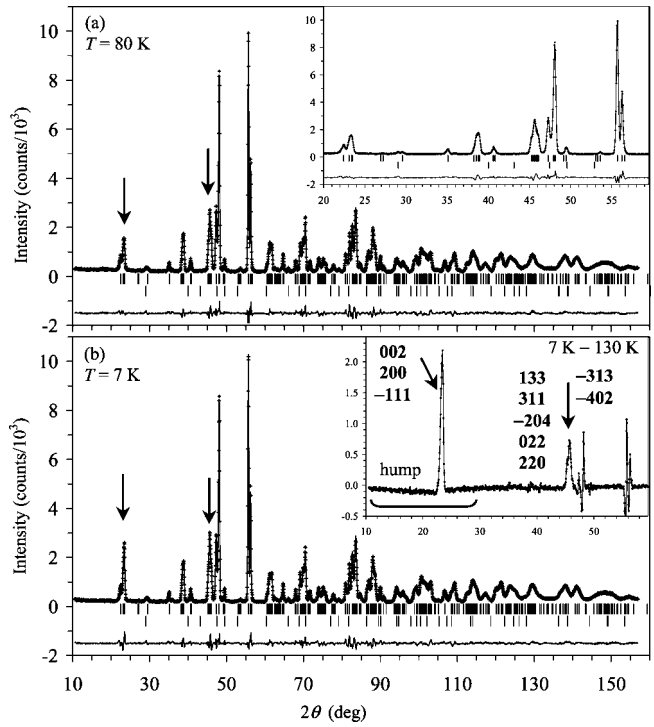

Figure 2. Observed (crosses), calculated (solid line), and difference patterns resulting from the Rietveld analysis of neutron powder diffraction data for $BiCrO_3$ at (a) 80 K and (b) 7 K. Bragg reflections are indicated by tick marks. The lower tick marks are given for reflections from Cr_2O_3. The inset in panel a depicts the enlarged fragment. The inset in panel b shows the difference pattern obtained by subtracting the experimental pattern at 130 K from that at 7 K and emphasizes the magnetic reflections and hump between 10 and 30° at 130 K. Indices of magnetic reflections are given. Arrows are attached to the strongest magnetic reflections.

indexed with the same lattice parameters as the chemical cell. Therefore, the three-dimensional long-range ordered magnetic structure can be described in terms of a propagation vector $\mathbf{k} = (0, 0, 0)$, and we determined the crystal structures and magnetic moments assuming one phase with space group *C*2/*c*. Magnetic moments of Cr^{3+} were found to align along the monoclinic *b* axis, similar to the direction of magnetic moments of Mn^{3+} in $BiMnO_3$.[18,25] Because $BiCrO_3$ is a (canted) antiferromagnet,[21,29,30] the following linear constraint was imposed on the magnetic moments, μ, of the Cr sites: $\mu(Cr1) = -\mu(Cr2)$. Attempts to refine the canting angle (using a different program) failed because of a very weak ferromagnetic moment (about $0.015\mu_B$ at 5 K).[30] Unconstrained refinement ($\mu(Cr1) \neq -\mu(Cr2)$) also did not improve the fit and *R* factors. Therefore, the G-type[38] antiferromagnetic model is a very good approximation of the magnetic structure of $BiCrO_3$. We note that the symmetry allows spin canting at the Cr2 site, giving a weak ferromagnetic component along the *b* axis.

To check for the possibility of deviation from stoichiometry, we refined the occupancies, *g*, of all the sites using the neutron diffraction data measured at all the temperatures. All the *g* parameters were very close to unity. For example, at 130 K, the refinement of the *g* parameters for oxygen atoms together with other variable parameters (except for *B*(O1), *B*(O2), and *B*(O3) because of correlations with *g*)

(38) Wollan, E. O.; Koehler, W. C. *Phys. Rev.* **1955**, *100*, 545.

Table 3. Structure Parameters of $BiCrO_3$ at 7, 50, 80, and 130 K[a]

site	Wyckoff position	*x*	*y*	*z*	*B* (Å^2)
Bi	8*f*	0.13388(16)	0.2129(3)	0.13076(18)	0.18(4)
		0.13391(17)	0.2131(3)	0.13075(18)	0.28(4)
		0.13336(16)	0.2130(3)	0.13107(17)	0.34(4)
		0.13324(16)	0.2134(3)	0.13098(17)	0.34(3)
Cr1	4*e*	0	0.2410(7)	0.75	0.39(10)
		0	0.2415(8)	0.75	0.47(11)
		0	0.2412(7)	0.75	0.53(10)
		0	0.2409(7)	0.75	0.43(10)
Cr2	4*d*	0.25	0.25	0.5	0.49(11)
		0.25	0.25	0.5	0.35(11)
		0.25	0.25	0.5	0.41(10)
		0.25	0.25	0.5	0.44(10)
O1	8*f*	0.0874(3)	0.2017(5)	0.5878(3)	0.75(5)
		0.0864(3)	0.2018(5)	0.5872(3)	0.75(6)
		0.0867(3)	0.2009(5)	0.5874(2)	0.68(5)
		0.0871(3)	0.2012(5)	0.5877(2)	0.78(5)
O2	8*f*	0.1542(3)	0.5272(5)	0.3650(3)	0.47(5)
		0.1536(3)	0.5274(5)	0.3649(3)	0.47(5)
		0.1537(3)	0.5268(5)	0.3648(3)	0.51(5)
		0.1547(3)	0.5272(5)	0.3651(3)	0.58(5)
O3	8*f*	0.3571(3)	0.5213(5)	0.1581(3)	0.31(5)
		0.3572(3)	0.5211(5)	0.1584(3)	0.34(5)
		0.3570(3)	0.5217(5)	0.1581(3)	0.33(5)
		0.3570(3)	0.5223(5)	0.1580(3)	0.24(5)

[a] Space group *C*2/*c* (No. 15); $Z = 8$. Occupation of all sites is unity. The first (*x*, *y*, *z*, and *B*) line of each site is for 7 K, the second line is for 50 K, the third line is for 80 K, and the fourth line is for 130 K. 7 K: $a = 9.4641(4)$ Å, $b = 5.4790(2)$ Å, $c = 9.5850(4)$ Å, $\beta = 108.568(3)°$, and $V = 471.15(3)$ Å^3; $R_{wp} = 7.43\%$ ($S = R_{wp}/R_e = 1.73$), $R_p = 5.68\%$, $R_B = 1.26\%$, and $R_F = 0.64\%$; $\mu = 2.55(2)\mu_B$. 50 K: $a = 9.4621(4)$ Å, $b = 5.4783(2)$ Å, $c = 9.5832(4)$ Å, $\beta = 108.569(3)°$, and $V = 470.90(3)$ Å^3; $R_{wp} = 7.64\%$ ($S = 1.76$), $R_p = 5.89\%$, $R_B = 1.99\%$, and $R_F = 0.96\%$; $\mu = 2.43(2)\mu_B$. 80 K: $a = 9.4620(4)$ Å, $b = 5.4781(2)$ Å, $c = 9.5835(3)$ Å, $\beta = 108.568(3)°$, and $V = 470.89(3)$ Å^3; $R_{wp} = 7.16\%$ ($S = 1.65$), $R_p = 5.56\%$, $R_B = 1.70\%$, and $R_F = 0.80\%$; $\mu = 2.09(2)\mu_B$. 130 K: $a = 9.4658(5)$ Å, $b = 5.4810(2)$ Å, $c = 9.5879(4)$ Å, $\beta = 108.564(3)°$, and $V = 471.56(3)$ Å^3; $R_{wp} = 7.03\%$ ($S = 1.65$), $R_p = 5.44\%$, $R_B = 1.60\%$, and $R_F = 0.71\%$.

gave $g(O1) = 0.990(6)$, $g(O2) = 0.998(6)$, and $g(O3) = 1.007(6)$. The refinement of the *g* parameters for Bi and Cr atoms together with other variable parameters (except for *B*(Bi), *B*(Cr1), and *B*(Cr2)) resulted in $g(Bi) = 1.004(5)$, $g(Cr1) = 0.999(13)$, and $g(Cr2) = 0.990(13)$. These facts support no noticeable deviation from the stoichiometry of $BiCrO_3$. The *g* values were therefore fixed at unity for all the sites in the subsequent Rietveld refinements.

Table 3 gives lattice parameters, *R* factors, fractional coordinates, *B* parameters, and refined magnetic moments in the monoclinic phase. Bond lengths, angles, and BVS are listed in Table 4. Figures 1b and 2 display observed, calculated, and difference neutron diffraction patterns.

The neutron diffraction data unambiguously prove that $BiCrO_3$ has antiferromagnetic long-range order below $T_N = 109$ K. The magnetic structure is very simple with magnetic moments coupled antiferromagnetically in all directions, forming the so-called G-type antiferromagnetic structure (Figure 3).[38] Note that the magnetic structure found in $BiCrO_3$ was predicted from first-principles electronic-structure calculations.[39] Isotropic antiferromagnetic interactions are expected for nongenerated magnetic ions such as Cr^{3+} ($S = 3/2$, where *S* is spin). The G-type antiferromagnetic structure is also found in other chromites such as $LaCrO_3$ and $YCrO_3$ having an orthorhombic $GdFeO_3$-type structure.[40]

Table 4. Selected Bond Lengths (*l*, Å), Angles (deg), and BVS in $BiCrO_3$ at 7, 50, 80, and 130 K[a]

	7 K	50 K	80 K	130 K
Bi−O2	2.238(3)	2.242(3)	2.248(3)	2.241(3)
Bi−O3	2.257(3)	2.256(3)	2.252(3)	2.254(3)
Bi−O1	2.325(3)	2.329(3)	2.323(3)	2.326(3)
Bi−O1a	2.446(3)	2.437(3)	2.439(3)	2.443(3)
Bi−O3a	2.652(3)	2.650(3)	2.656(3)	2.659(3)
Bi−O2a	2.787(3)	2.787(3)	2.782(3)	2.783(3)
Bi−O3b	2.911(3)	2.911(3)	2.905(3)	2.904(3)
Bi−O2b	2.978(3)	2.975(3)	2.982(3)	2.982(3)
Bi−O3c	3.077(3)	3.079(3)	3.083(3)	3.085(3)
Bi−O1b	3.150(3)	3.158(3)	3.157(3)	3.155(3)
BVS(Bi)	2.95	2.95	2.95	2.94
Cr1−O1 (×2)	1.991(3)	1.991(3)	1.991(3)	1.991(3)
Cr1−O2 (×2)	1.983(4)	1.977(4)	1.981(4)	1.988(4)
Cr1−O3 (×2)	1.978(4)	1.977(4)	1.980(4)	1.983(4)
BVS(Cr1)	2.97	2.99	2.97	2.95
Cr2−O1 (×2)	1.993(3)	1.997(3)	1.996(3)	1.996(3)
Cr2−O2 (×2)	2.014(3)	2.016(3)	2.014(3)	2.013(3)
Cr2−O3 (×2)	1.979(3)	1.981(3)	1.977(3)	1.975(3)
BVS(Cr2)	2.88	2.86	2.88	2.89
Cr1−O1−Cr2 (×2)	152.1(1)	151.6(1)	151.7(1)	151.9(1)
Cr1−O2−Cr2 (×2)	160.3(1)	160.5(1)	160.5(1)	160.0(1)
Cr1−O3−Cr2 (×2)	155.8(1)	155.7(1)	155.7(1)	155.8(1)

[a] $BVS = \Sigma_{vi=1}^{N}$, $v_i = \exp[(R_0 - l_i)/B]$, where *N* is the coordination number, $B = 0.37$, $R_0(Bi^{3+}) = 2.094$, and $R_0(Cr^{3+}) = 1.724$.

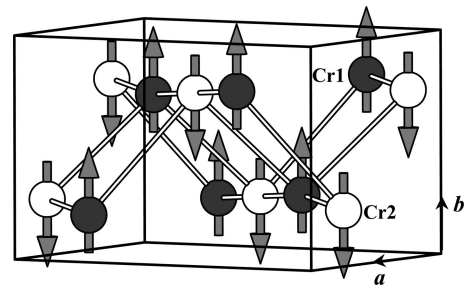

Figure 3. Crystal structure of $BiCrO_3$ with solid lines displaying the unit (chemical and magnetic) cell. Arrows show the direction of the magnetic moments below $T_N = 109$ K.

However, there are some features in magnetic properties of $BiCrO_3$ that have to be explained. First, there is a relatively large difference (~3 times) between $T_N = 109$ K and Curie−Weiss temperature θ obtained from the Curie−Weiss fit of magnetic susceptibilities ($\theta = -301$ and -359 K).[21,30] This difference indicates the presence of magnetic frustration. Second, there are deviations of the inverse magnetic susceptibilities from the linear Curie−Weiss behavior far above T_N and tendency to form broad maxima.[30] This behavior is an indication of the presence of short-range correlations or low dimensionality.

Noticeable differences between T_N and θ also were found in orthorhombic $YCrO_3$ ($T_N = 141$ K and $\theta = -230$ and -360 K)[41,42] and $LuCrO_3$ ($T_N = 115$ K and $\theta = -274$ K).[42] The interactions between Cr^{3+} ions should be rather isotropic in the orthorhombic phases because the difference in the Cr−O−Cr angles is small (e.g., 145.58 and 144.28° in

(39) Hill, N. A.; Battig, P.; Daul, C. *J. Phys. Chem. B* **2002**, *106*, 3383.

(40) (a) Bertaut, E. F.; Bassi, G.; Buisson, G.; Burlet, P.; Chappert, J.; Delapalme, A.; Mareschal, J.; Roult, G.; Aleonard, R.; Pauthenet, R.; Rebouillat, J. P. *J. Appl. Phys.* **1966**, *37*, 1038. (b) Bertaut, E.; Mareschal, J.; De Vries, G.; Aleonard, R.; Pauthenet, R.; Rebouillat, J.; Zarubicka, V. *IEEE Trans. Magn.* **1966**, *2*, 453.

(41) Tsushima, K.; Aoyagi, K.; Sugano, S. *J. Appl. Phys.* **1970**, *41*, 1238.

(42) (a) Sahu, J. R.; Serrao, C. R.; Rao, C. N. R. *Solid State Commun.* **2008**, *145*, 52. (b) Lal, H. B.; Gaur, K.; Dwivedi, R. D. *J. Mater. Sci. Lett.* **1995**, *14*, 9.

$YCrO_3$ and 159.07 and 161.36° in $LaCrO_3$).[36,43] Therefore, the origin of magnetic frustration (or large difference between T_N and θ) in $YCrO_3$ and also $BiCrO_3$ should lie in the effect of next nearest-neighbor (NNN) interactions.[41] It is known that NNN interactions play a major role in the physical properties of orthorhombic manganites $RMnO_3$ (R = La to Lu and Y).[44]

The strength of the NN interaction should strongly depend on the Cr−O−Cr bond angles. In the monoclinic phase of $BiCrO_3$, the variation of the Cr−O−Cr bond angles is large (from 152 to 160°; see Table 4). Therefore, some antiferromagnetic interactions (through Cr1−O1−Cr2) should be weaker than others forming quasi-two-dimensional layers. These structural features of monoclinic $BiCrO_3$ may explain the observed low-dimensional magnetic properties above T_N.[30] Magnetic correlations are developed above T_N as can be seen from a very broad hump between 10 and 30° in the neutron diffraction pattern at 130 K (the presence of this hump is more clearly seen on the (7−130 K) difference pattern given in the inset of Figure 2b (see also the Supporting Information)).

In the orthorhombic phase of $BiCrO_3$, the variation of the Cr−O−Cr bond angles is significantly reduced (152.6 and 153.9°) and becomes similar to those of other orthorhombic phases ($YCrO_3$, $LaCrO_3$, $RMnO_3$, and so on). Investigation of magnetic and dielectric properties of a stabilized (by different substitutions) orthorhombic phase of $BiCrO_3$ may be interesting because weakly biferroic properties were reported in $YCrO_3$ containing no ions with the lone electron pair.[43] For example, $Bi_{0.95}Y_{0.05}CrO_3$ already crystallizes in the $GdFeO_3$-type orthorhombic structure.[45]

Neutron diffraction data suggested that the global G-type antiferromagnetic structure is not changed below T_N. It seems that only tiny changes of the canting angle occur. However, it was impossible to refine the canting angle. Therefore, the neutron powder diffraction data cannot explain additional magnetic anomalies that have been observed below T_N.[30] The temperature dependence of the lattice parameters (see the Supporting Information) showed anomalies near 40 and 70 K in agreement with magnetization data.[30]

The crystal structure of $BiCrO_3$ is very well-described by the centrosymmetric *C*2/*c* model (below 420 K). Our results coupled with the electron diffraction results on bulk samples[20] and the observation of antiferroelectric properties in thin film samples[46] give strong evidence for the centrosymmetric crystal structure of $BiCrO_3$. Therefore, the observation of broad anomalies near 440 K on the dielectric constant of $BiCrO_3$ should be attributed to an antiferroelectric−paraeletric phase transition rather than to a ferroelectric−paraeletric transition.[21] Interpretation of dielectric anomalies sometimes is not straightforward. First, both ferroelectric and antiferroelectric materials show maxima on dielectric constants during the transition to a paraelectric state.[47] Second, relaxor-like maxima on dielectric constants with a strong frequency dependence (observed in $BiCrO_3$)[21] may appear due to defect-induced conductivity.[8,48]

The reduction in the observed magnetic moment even at 7 K ($2.55(2)\mu_B$) in comparison to the expected value of $3\mu_B$ for a Cr^{3+} ion ($S = 3/2$) may be ascribed to the covalency effect. In $RCrO_3$ (R = La to Lu and Y),[40] the magnetic moment of Cr^{3+} at 4.2 K varies between $2.45\mu_B$ and $2.96\mu_B$, showing no correlation with the size and nature of R^{3+} ions. The reduced magnetic moment as compared to the theoretical one also was found in $BiCoO_3$, $BiNiO_3$, and $BiMnO_3$.[14,18,27] To obtain information on the formal oxidation states of Bi and Cr, we calculated their bond valence sums (Tables 2 and 4).[37] The resulting BVS values are very close to +3 in the monoclinic phase. However, we should emphasize that the BVS value for Bi in the orthorhombic phase is noticeably reduced (+2.76), indicating the underbonding of Bi^{3+}.

In conclusion, using neutron diffraction, we obtained accurate structural parameters of $BiCrO_3$ in a wide temperature range above and below the structural and magnetic phase transitions. The G-type magnetic structure is realized in $BiCrO_3$, and the magnetic structure does not change from 109 K down to 7 K.

Acknowledgment. This work was supported by the World Premier International Research Center Initiative (WPI Initiative, MEXT, Japan) and by the NIMS Individual-Type Competitive Research Grant. This work was performed under the NIMS-RIKEN-JAEA Cooperative Research Program on Quantum Beam Science and Technology.

Supporting Information Available: Experimental, calculated, and difference neutron powder diffraction patterns of $BiCrO_3$ at 50 K (Figure S1), temperature dependence of lattice parameters (Figure S2), and details of difference neutron powder diffraction patterns (Figure S3) (PDF). This material is available free of charge via the Internet at http://pubs.acs.org.

CM800375D

(43) Ramesha, K.; Llobet, A.; Proffen, T.; Serrao, C. R.; Rao, C. N. R. *J. Phys.: Condens. Matter* **2007**, *19*, 102202.
(44) (a) Kimura, T.; Ishihara, S.; Shintani, H.; Arima, T.; Takahashi, K. T.; Ishizaka, K.; Tokura, Y. *Phys. Rev. B: Condens. Matter Mater. Phys.* **2003**, *68*, 60403. (b) Tachibana, M.; Shimoyama, T.; Kawaji, H.; Atake, T.; Takayama-Muromachi, E. *Phys. Rev. B: Condens. Matter Mater. Phys.* **2007**, *75*, 144425.
(45) Belik, A. A.; Takayama-Muromachi, E., unpublished work.
(46) Kim, D. H.; Lee, H. N.; Varela, M.; Christen, H. M. *Appl. Phys. Lett.* **2006**, *89*, 162904.
(47) Stefanovich, S. Y.; Belik, A. A.; Azuma, M.; Takano, M.; Baryshnikova, O. V.; Morozov, V. A.; Lazoryak, B. I.; Lebedev, O. I.; Van Tendeloo, G. *Phys. Rev. B: Condens. Matter Mater. Phys.* **2004**, *70*, 172103.
(48) Scott, J. F. *J. Mater. Res.* **2007**, *22*, 2053.